Radiolytic degradation of hydrophilic PyTri ligands for minor actinide recycling

Eros Mossini Correspondent[1], Elena Macerata[1], Luigi Brambilla[2], Walter Panzeri[3], Andrea Mele[2,3], Chiara Castiglioni[2], Mario Mariani[1] Co-Authors

[1] *Department of Energy, Politecnico di Milano, Piazza L. da Vinci 32, I-20133 Milano, Italy*

[2] *Department of Chemistry, Materials and Chemical Engineering, Politecnico di Milano, Piazza L. da Vinci 32, I-20133 Milano, Italy*

[3] *C.N.R. – Consiglio Nazionale delle Ricerche, Istituto di Chimica del Riconoscimento Molecolare, Sezione "U.O.S. Milano Politecnico", Via L. Mancinelli 7, I-20131 Milano, Italy*

Abstract

The 2,6-bis[1H-1,2,3-triazol-4-yl]-pyridine (PyTri) chelating unit has already shown promising properties for application to advanced hydrometallurgical processes aimed at recovering minor actinides from highly active raffinate. Radiolytic stability is an undeniable key requirement for chemicals involved in highly radioactive solutions partitioning, since radiolysis can have a huge impact on system safety and performances.

In this work, the radiolytic degradation of two hydrophilic PyTri complexing agents was investigated by different analytical techniques. The radiation damage was delivered by a ^{60}Co source. The main radiation-induced ligand degradation by-products were hypothesized. Unprecedented PyTri ligands radiolytic stability was proved, further recommending their implementation in future partitioning processes.

Keywords

FT-Raman; ESI-MS; *i*-SANEX; PyTri ligands; Radiolysis; Minor Actinides Partitioning

Introduction

Sustainability and public acceptance of the nuclear industry could be improved by a spent nuclear fuel (SNF) management strategy that recovers reusable actinide (An), *i.e.* uranium and transuranium elements [1-2]. In fact, important improvement of natural resources exploitation and environmental footprint of final waste repository could be achieved by U and Pu multi-recycling along with minor actinides (MA: Np, Am, Cm) Partitioning followed by Transmutation (P&T strategy) in proper fast nuclear reactors [3-6]. This strategy entails MA separation from neutronic poisons, the lanthanides (Ln) among all, and is hindered by the similar chemical behavior of trivalent MA and Ln along with the unfavorable mass ratio in the waste [7]. Worldwide, promising counter-current multistage hydrometallurgical processes have been proposed to recycle trivalent MA [8-11]. Within the last Framework Programs (from FP3 to FP7), the European Commission funded joint research projects to develop safe, compact and simplified separation strategies [8,12,13]. A promising process, named innovative-Selective ActiNide EXtraction (*i*-SANEX), based on two extraction cycles was proposed for the direct trivalent MA recovery from the Plutonium and URanium EXtraction (PUREX) raffinate [14-16]. In the first step, a lipophilic extractant is employed to extract MA and Ln from an acidic aqueous feed containing also other fission and corrosion products. Among all, *N,N,N',N'-Tetraoctyl Diglycolamide* (TODGA) is endowed with high MA and Ln affinity combined with satisfactory radiochemical stability [17-19]. In the second cycle, the trivalent MA are selectively separated from the Ln by back-extraction into an aqueous phase by a hydrophilic complexing agent. Great efforts have been driven to develop water-soluble ligands pursuing several industrial constraints: *i)* affinity for MA and selectivity towards Ln; *ii)* reversibility of MA retention; *iii)* fast complexation kinetics; *iv)* no hydrodynamic problems; *v)* stability towards hydrolysis and radiolysis; *vi)* CHON principle [20]. A chemical in compliance with the CHON principle contains just C, H, O and N atoms in order to be completely incinerable without leaving secondary solid waste legacy. The fulfilment of all requirements is a challenging key issue

concerning the technical feasibility and success of the P&T strategy. To date, several hydrophilic ligands have been developed, but none of them has fully matched all the constraints [21-23]. In particular, the resistance towards hydrolysis and radiolysis is an undeniable key requirement in view of the scale-up of advanced SNF partitioning processes owing to the significant radionuclides content in the PUREX raffinate [24-25]. In fact, radiolysis may induce production of diluent and ligand by-products, leading to degradation of the original ligand and to potential alteration of several properties [26-27]. Furthermore, radiation-induced alterations would undesirably affect not only the separation efficiency, but also the physico-chemical properties of the solvent [28]. In particular, the change of density and viscosity and the formation of precipitates and third phases have to be investigated, since they may compromise the hydrodynamic stability of the system or else the safety of the future reprocessing plants, due to malfunctioning at the pumps and at the centrifuges [29-31]. Great efforts have been devoted to study the radiolytic stability of lipophilic extractants, in particular TODGA, and now both degradation mechanism and separation performances are rather known [32-35]. Some modifications of the ligand structure have been attempted in order to enhance its radiochemical stability, *i.e.* by adding methyl groups in methylene carbon positions [35-37]. Contrariwise to the lipophilic counterpart, poor literature information exists concerning the radiolytic behavior of hydrophilic complexing agents to be used for the MA selective stripping. So far, discordant results have been obtained on the radiation resistance of the non-CHON compliant *Bis(di-sulfo-Phenyl)-Triazine-Pyridine* (SO_3-Ph-BTP), former *i*-SANEX reference hydrophilic ligand for MA back-extraction [38-39].

In this paper, two CHON hydrophilic complexing agents have been studied: *2,6-bis[1-(propan-1-ol)-1,2,3-triazol-4-yl)]pyridine* (PyTri-Diol, see Figure 1, *Left*) and *2,6-bis[1-(propan-1,2-diol)-1,2,3-triazol-4-yl)]pyridine* (PyTri-Tetraol, see Figure 1, *Right*).

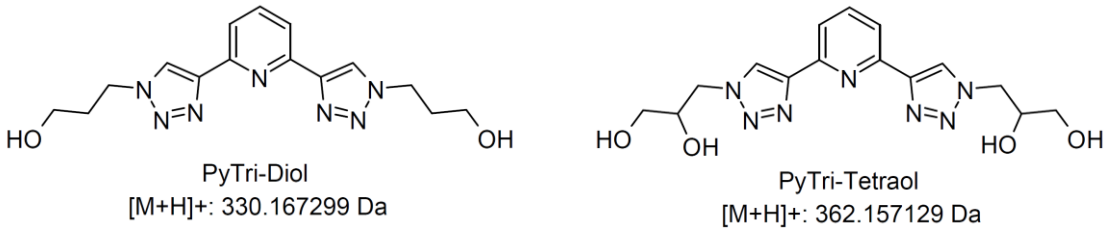

Figure 1 Molecular structures of PyTri-Diol and PyTri-Tetraol.

The common *2,6-bis[1H-1,2,3-triazol-4-yl]-pyridine* (PyTri) chelating unit has already shown promising properties for the application to advanced hydrometallurgical processes aimed at recovering An from highly active raffinates [40-42]. In particular, the water-soluble PyTri-Diol, owing to successful single stage centrifugal contactor experiment proving its effectiveness in separating trivalent MA from Ln, has been recently promoted as new *i*-SANEX reference ligand [43-44]. Even if preliminary batch liquid-liquid extraction tests have already suggested promising hydrolytic and radiolytic stability of aqueous stripping solvent based on PyTri-Diol or PyTri-Tetraol, further investigations are required [40]. The aim of this paper is to shine a light on this aspect. In order to simulate the radiolytic damage delivered at reprocessing conditions, stripping solutions containing the hydrophilic ligand were irradiated at different absorbed doses by means of a ^{60}Co gamma source (with 2.5 kGy/h dose rate) and subsequently analyzed. Even though the radiation damage of MA stripping solvents would mainly be caused by alpha emitters, the irradiation is usually performed by gamma sources [26]. As justification of this choice, the use of gamma rays is technically simpler and the results more conservative than employing alpha irradiation [27]. The investigation has been mainly focused on the identification of the main radiation-induced ligand by-products by means of Fourier Transformed (FT)-Raman spectroscopy and Electrospray Ionization Mass Spectrometry (ESI-MS).

Experimental

Reagents and materials

Analytical grade reagents were purchased from Sigma Aldrich and used without further purification. PyTri-Diol and PyTri-Tetraol complexing agents were synthetized at

Università di Parma according to the procedures elsewhere described [40]. The stripping solutions consisted of 0.08 mol/L PyTri-Diol or 0.15 mol/L PyTri-Tetraol dissolved in 0.44 mol/L HNO_3, as optimized in previous works [40, 44].

Ageing and irradiation conditions

PyTri-Diol and PyTri-Tetraol stripping solutions were prepared as above described, stored in 4 mL glass vials, closed with a plastic lid and sealed with Parafilm® in order to avoid any sample leakage during irradiation. The stripping solutions were not pre-equilibrated with the organic phase. Between the preparation and the analysis, the samples were kept in the dark. The irradiations were performed at ambient temperature (23±2°C) by a ^{60}Co gamma source with 2.5 kGy/h dose rate. For both ligands, a reference solution was not irradiated, but just aged for the same length of time. At the end of the irradiation of the sample with highest absorbed dose, all samples were stored in the dark at 4±1°C until further analysis. Therefore, same thermal treatment was operated for all samples. In order to evaluate ageing and radiolysis effects, about 200 µL aliquots were subsampled and transferred into NMR quartz tubes for FT-Raman spectroscopy. Similarly, 10 µL aliquots of aged and irradiated solutions were sampled, properly diluted with methanol and analyzed by ESI-MS.

ESI-MS conditions

ESI-MS spectra were acquired on a Bruker Esquire 3000 PLUS instrument (ESI Ion Trap LC/MSn System), equipped with an ESI source and a quadrupole ion trap detector (QIT). PyTri-Diol and PyTri-Tetraol samples were diluted in methanol to 10^{-2} g/L before being directly infused in the ESI-MS at 4 µL/min rate. After each experiment, both syringe and loop used for the infusion were abundantly rinsed with methanol in order to avoid sample cross-contaminations. The analyses were performed in positive ion mode after optimization of the acquisition parameters: 4.5 kV needle voltage, 10 L/h N^2 flow rate, 40 V cone voltage, trap drive set to 46, 115.8 V capillary exit, 13000 (*m/z*)/s scan resolution over the 35–900 *m/z* mass/charge range. The signals of pristine ligand and by-products (both proton and sodium adducts) were identified in the spectra of fresh, aged and irradiated solutions. The assignment of some detected by-products was confirmed by

collision-activated decomposition (CID) tandem mass spectrometry experiments (MS^2), with an isolation width of 1 mass unit and a duly optimized collisional fragmentation amplitude between 0.5 and 1.00 V (see *Supplementary Information* for further details, ESI-MS^2 spectra and fragments tentative assignment). All data were analyzed using *Bruker Daltonics Data Analysis* software (version 5.1, 2002).

FT-Raman conditions

FT-Raman spectra were recorded by means of a Thermo Scientific NXR9650 FT-Raman spectrometer, equipped with a 1064 nm Nd:YVO_4 laser. Spectra of liquid samples placed in NMR quartz tubes were collected in back-scattering geometry with the following parameters: 512 scans, 4 cm^{-1} resolution, 500 mW exciting laser power. The analyses were performed between 50 and 3700 cm^{-1}. In order to perform a semi-quantitative evaluation of ligand consumption, the calibration was obtained by acquiring spectra of fresh ligand solutions by dilution. In particular, solutions with PyTri-Diol concentrations ranging from 0.02 mol/L to 0.08 mol/L and PyTri-Tetraol from 0.04 mol/L to 0.15 mol/L were analyzed. Only the main peaks in the spectrum were analyzed. The calibration was performed on the net area of each peak by linear regression (see *Supplementary Information* for calibration details) [45]. The uncertainties were derived taking into account the signal to noise ratio. All data were analyzed using *Thermo Scientific Omnic* software (version 7.1, 2004).

DFT simulations

For both ligands, geometry was optimized by Density Functional Theory (DFT) with the hybrid B3LYP correlation functional [46-47] and the 6-311G(d,p) basis set [48] implemented in the Gaussian 09 code package [49]. Afterwards, Raman spectra calculations were carried out at the same level of theory for the optimized geometries. First, the calculations were performed in the gas phase. Then, the effects of the solvent (water) were taken into account using the *SCRF(PCM,Solvent=Water)* keyword [50]. Finally, in addition to force constants and resulting vibrational frequencies, the *Freq=Raman* keyword allowed to calculate the Raman intensities.

Results and discussion

FT-Raman

The Raman bands identification was performed on the basis of DFT simulations. In Figure 2, the experimental Raman spectra of PyTri-Diol and PyTri-Tetraol are compared with the corresponding simulated ones in the 700-2000 cm^{-1} Raman shift range.

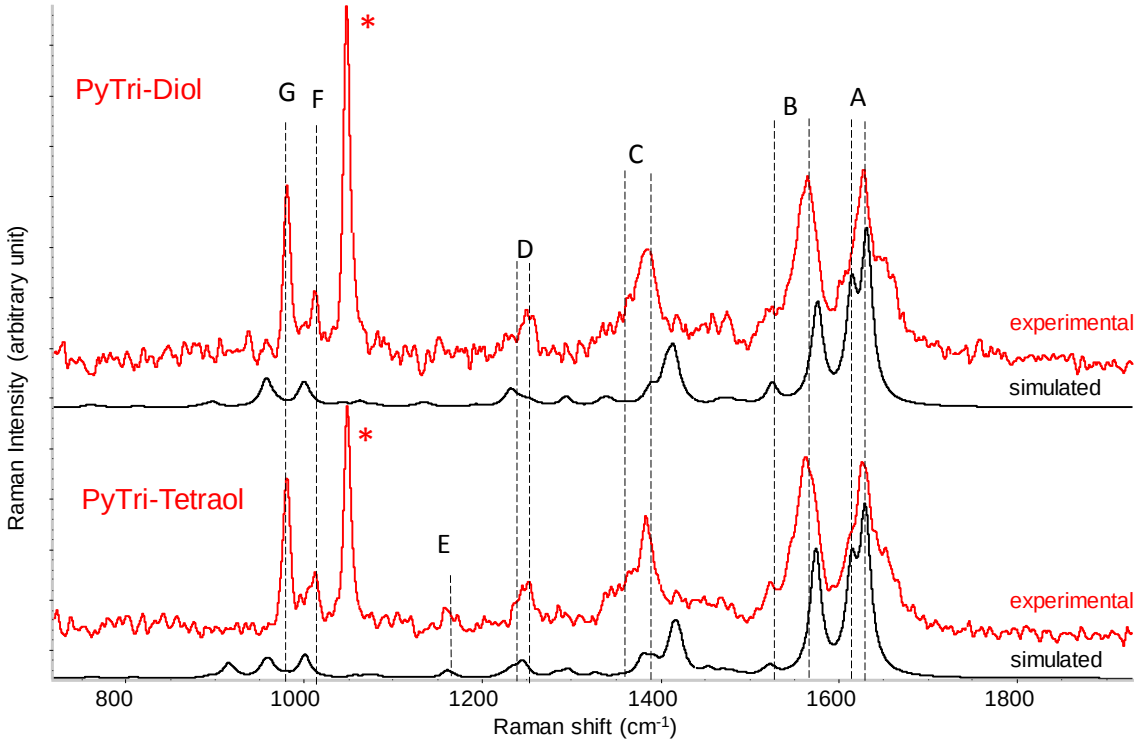

Figure 2 Experimental (red lines) and simulated with Gaussian 09 (black lines) Raman spectra of PyTri-Diol and PyTri-Tetraol in the range 700-2000 cm^{-1}. From *Top* to *Bottom*: experimental spectrum of fresh 0.08 mol/L PyTri-Diol in 0.44 mol/L HNO_3 solution; simulated spectrum of PyTri-Diol; experimental spectrum of fresh 0.15 mol/L PyTri-Tetraol in 0.44 M HNO_3 solution; simulated spectrum of PyTri-Tetraol. All experimental spectra are normalized, and baseline corrected. Lines discussed in the text are labelled from A to G.

As it could be observed, the experimental Raman spectra of fresh PyTri-Diol and PyTri-Tetraol present a similar spectral pattern except for the band E which is characteristic of PyTri-Tetraol sample. The nitrate anion signal at 1046 cm^{-1} is marked

with a red star in the experimental FT-Raman spectra of Figure 2). A satisfactory reproduction of the experimental spectra has been achieved by DFT simulations. Clearly, the band at 1046 cm^{-1} is not present in the simulated spectra as it belongs to the nitrate anion and the simulations were performed with pure water as solvent. At the same time, the identification of the signals with lower Raman intensity could have been hindered by the not-negligible noise of the acquired spectra. A tentative vibrational assignment based on DFT simulation and curve fitting analysis performed on experimental PyTri-Diol and PyTri-Tetraol FT-Raman spectra (see *Supplementary Information* for fitting analysis details) is reported in Table 1. All signals observed in the experimental spectrum between 700 and 2000 cm^{-1} are referred to vibrations of C-H, C-C and C-N bonds mainly belonging to the aromatic moiety of the ligand.

Table 1 Tentative assignment of PyTri-Diol (first value, PTD) and PyTri-Tetraol (second value, PTT) principal Raman bands based on DFT simulations and curve fitting analysis.

Simulated Raman shifts [cm^{-1}] (PTD – PTT)	**Tentative assignment**	**Experimental Raman shifts [cm^{-1}] (PTD – PTT)**	**Tag**
1630 - 1628	Symmetric pyridinic C-C stretching	1650 - 1655	***Peak A***
1614 - 1614	Antisymmetric pyridinic C-N stretching	1625 - 1626	
1575 - 1573	Symmetric triazolyl C-C stretching	1562 - 1563	***Peak B***
1524 - 1522	Antisymmetric triazolyl C-C stretching	1521 - 1523	
1408 - 1416	Symmetric pyridinic C-N stretching	1382 - 1384	***Peak C***
1389 - 1381	Pyridinic C-N bending	1337 - 1349	
1253 - 1244	Symmetric triazolyl N-N stretching	1250 - 1288	***Peak D***
1231 - 1232	Antisymmetric triazolyl N-N stretching	1227 - 1248	
1158	Triazolyl N=N and C-C stretching (PyTri-Tetraol)	1160	***Peak E***
999 - 999	Pyridinic breathing	1010 - 1008	***Peak F***
956 - 957	Antisymmetric pyridinic C-H out of plane	980 - 979	***Peak G***

In order to shine a light on the radiolytic stability of PyTri-Diol and PyTri-Tetraol, solutions containing the hydrophilic complexing agents were irradiated by a 2.5 kGy/h dose rate ^{60}Co source at integrated absorbed dose of 25, 100 and 200 kGy and subsequently analyzed by FT-Raman technique. In fact, this value is coherent with the absorbed dose a stripping solution should undergo in case of unlikely continuous recycling for about two years of *i*-SANEX process operations [51]. For both ligands, a

non-irradiated solution was aged for the same length of time (40 days) and kept as reference in order to discriminate the effect of ageing from that of radiolysis. Furthermore, some ligands solutions were freshly prepared as blank and employed for the calibration by dilution. The acquired Raman spectra of fresh, aged and irradiated PyTri-Diol and PyTri-Tetraol solutions are reported in Figure 3 and Figure 4 respectively. An enlargement of 500 - 2000 cm^{-1} wavenumber range was considered, in order to better investigate the most relevant Raman signals. No evident alterations of fresh ligand signals are observable in aged and irradiated solutions. Furthermore, no new signals due to hydrolytic and radiolytic by-products are visible in the whole wavenumber range considered. As for the calibration, the net area of each peak was evaluated for aged and irradiated PyTri-Diol and PyTri-Tetraol solutions. Consequently, the concentration of the species preserving the Raman vibrational modes of each peak were calculated on the basis of the calibration. For sake of example, only the results of *Peak B* and *Peak C* are reported in Figure 5 and Figure 6 for PyTri-Diol and PyTri-Tetraol respectively. These two bands have been chosen as they are good representative of triazoles and pyridine moieties. In fact, *Peak B* was attributed to symmetric and antisymmetric triazolyl C-C stretching vibrations. On the other hand, *Peak C* was assigned to pyridinic C-N stretching and bending modes.

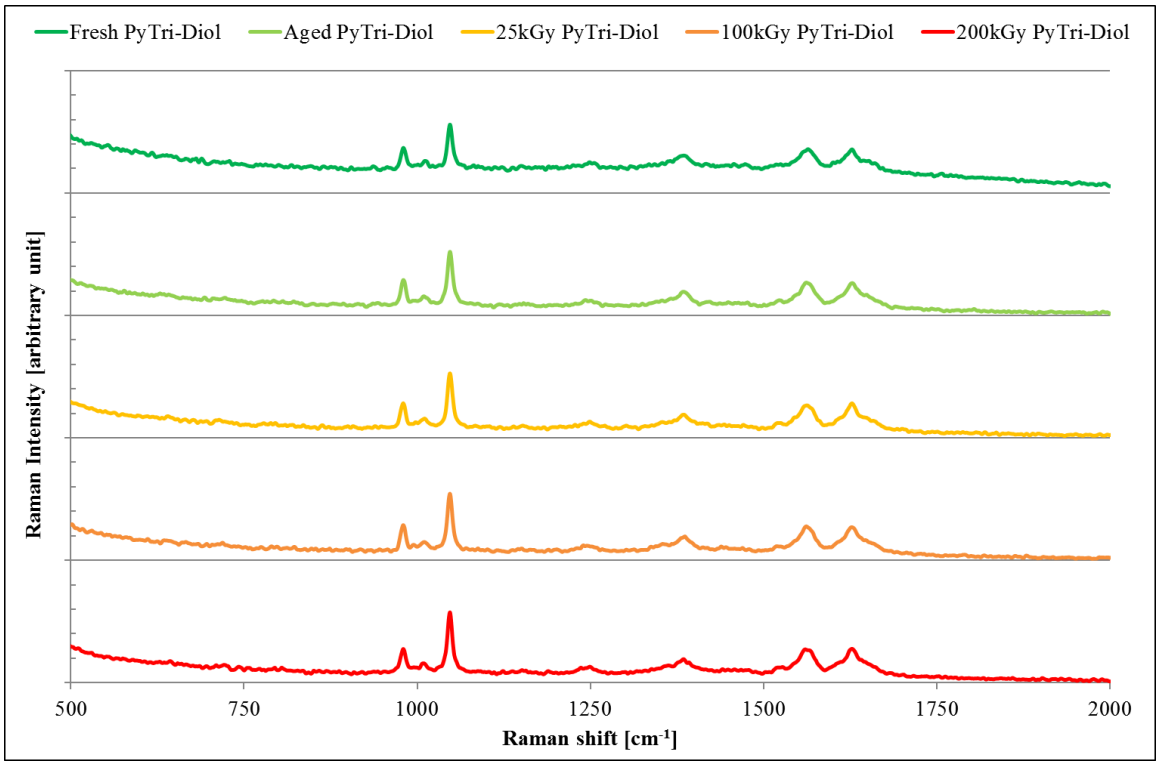

Figure 3 From *Top* to *Bottom*: 500 - 2000 cm^{-1} wavenumber range enlargement of FT-Raman spectra of fresh, aged and irradiated (at integrated dose of 25, 100, 200 kGy by the 2.5 kGy/h dose rate ^{60}Co source) 0.08 mol/L PyTri-Diol in 0.44 mol/L HNO_3 solutions are reported.

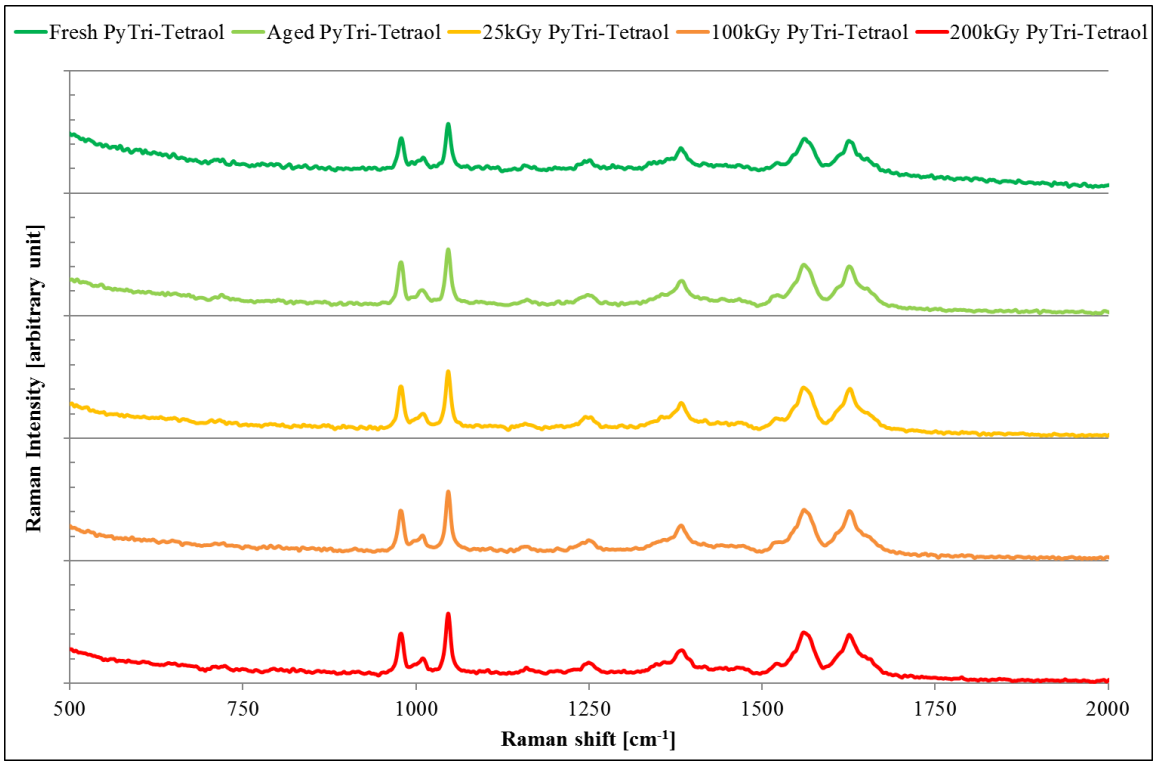

Figure 4 From *Top* to *Bottom*: 500 - 2000 cm^{-1} wavenumber range enlargement of FT-Raman spectra of fresh, aged and irradiated (at integrated dose of 25, 100, 200 kGy by the 2.5 kGy/h dose rate ^{60}Co source) 0.15 mol/L PyTri-Tetraol in 0.44 mol/L HNO_3 solutions are reported.

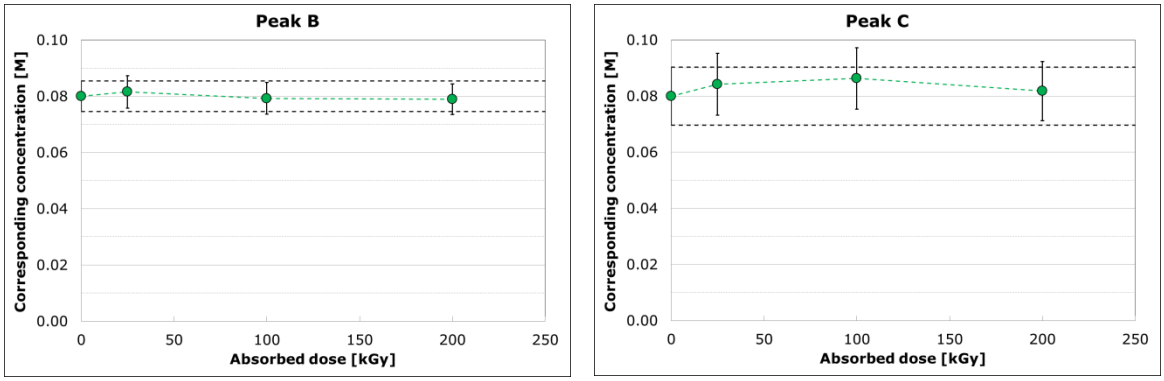

Figure 5 Concentration of species preserving the Raman vibration modes of *Peak B* (*Left*) and *Peak C* (*Right*), calculated from the respective calibration, in aged and irradiated (at integrated dose of 25, 100, 200 kGy) 0.44 mol/L HNO_3 solutions containing 0.08 mol/L PyTri-Diol.

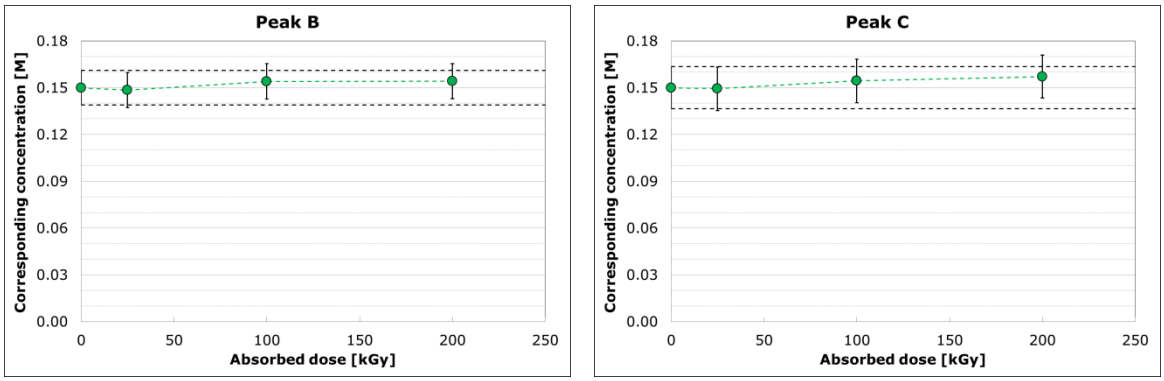

Figure 6 Concentration of species preserving the Raman vibration modes of *Peak B* (*Left*) and *Peak C* (*Right*), calculated from the respective calibration, in aged and irradiated (at integrated dose of 25, 100, 200 kGy) 0.44 mol/L HNO_3 solutions containing 0.15 mol/L PyTri-Tetraol.

As observable, the concentration of species preserving the Raman vibrational modes of *Peak B* and *Peak C* are unaltered for aged and irradiated solutions, within the not negligible (preferably improvable) experimental uncertainty. Analogous results were obtained for the other peaks and are reported in the *Supplementary Information*. These results suggest that the PyTri chelating unit should not be affected by hydrolytic and radiolytic degradation, since all the considered Raman bands are referred to vibrational modes belonging to the aromatic moiety of the ligands. Consequently, radiolytic by-products may reasonably present modifications just on the alkyl chains, with a preserved chelating unit. Therefore, in order to demonstrate that the extracting performances are unaltered both in terms of selectivity and efficiency, hydrophilicity of by-products must be verified, *i.e.* their detrimental transfer and accumulation in the organic solvent. These hypotheses would be in perfect agreement with the preliminary liquid-liquid extraction data obtained with aged and irradiated PyTri-Diol solutions [40].

ESI-MS

In order to corroborate the FT-Raman results, ESI-MS analyses were performed on fresh, aged (ageing of 40 days) and irradiated (integrated absorbed dose of 200 kGy with 2.5 kGy/h dose rate ^{60}Co source) PyTri-Diol and PyTri-Tetraol solutions. The chosen absorbed dose value is the same of the most irradiated solution analyzed by FT-Raman spectroscopy. For both ligands, ESI-MS spectra of aged solutions resulted to be unaltered

with respect to fresh ones (see *Supplementary Information*). Consequently, the effect of ageing can be neglected when analyzing irradiated solutions. On the other hand, slight differences were highlighted if comparing the spectra of fresh and irradiated PyTri-Diol and PyTri-Tetraol solutions, as shown in Figure 7 and Figure 8 respectively. The pristine ligands, present in protonated and sodiated forms, are, by far, the prevalent species also in irradiated solutions. Apart from few synthesis impurities observable also in the spectra of fresh ligand solutions, some new species attributable to radiolysis are present in irradiated solutions. In particular, as observable in Figure 7 (*bottom*), the main by-products of PyTri-Diol are: by-product ***1*** (proton adduct at *m/z* 272.1), by-product ***2*** (proton adduct at *m/z* 344.1), by-product ***3*** (proton adduct at *m/z* 360.1; sodium adduct at *m/z* 382.1), by-product ***4*** (proton adduct at *m/z* 391.2). The main by-products of PyTri-Tetraol (see Figure 8, *bottom*) are: by-product ***1*** (sodium adduct at *m/z* 310.1), by-product ***2*** (sodium adduct at *m/z* 414.1). The structures of these by-products (see Figure 9 and Figure 10 for PyTri-Diol and PyTri-Tetraol by-product structures respectively, see *Supplementary Information* for ESI-MS^2 spectra and fragments tentative assignment) were hypothesized on the basis of tandem mass spectrometry results.

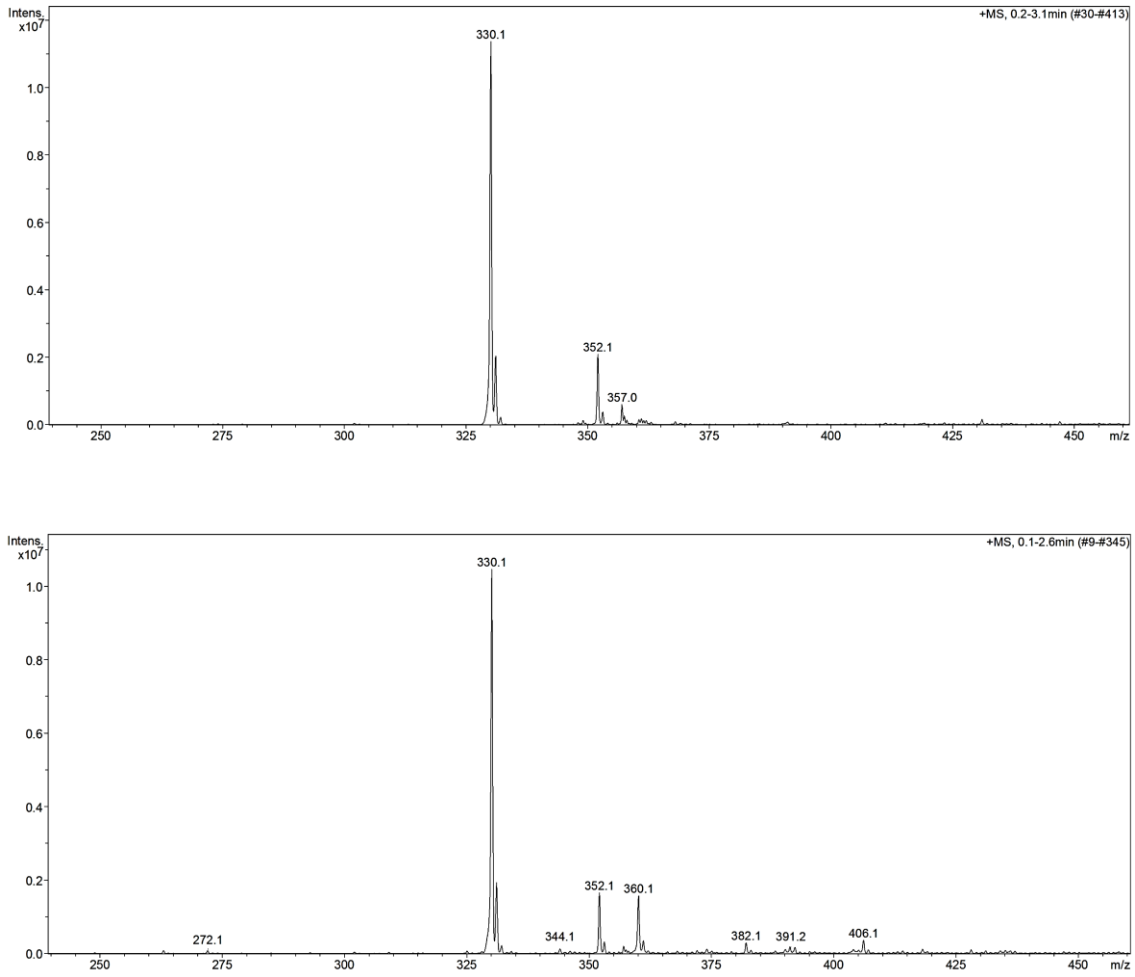

Figure 7 ESI-MS spectra of fresh (*Top*) and 200 kGy irradiated (*Bottom*) 0.44 mol/L HNO_3 solutions containing 0.08 mol/L PyTri-Diol solution.

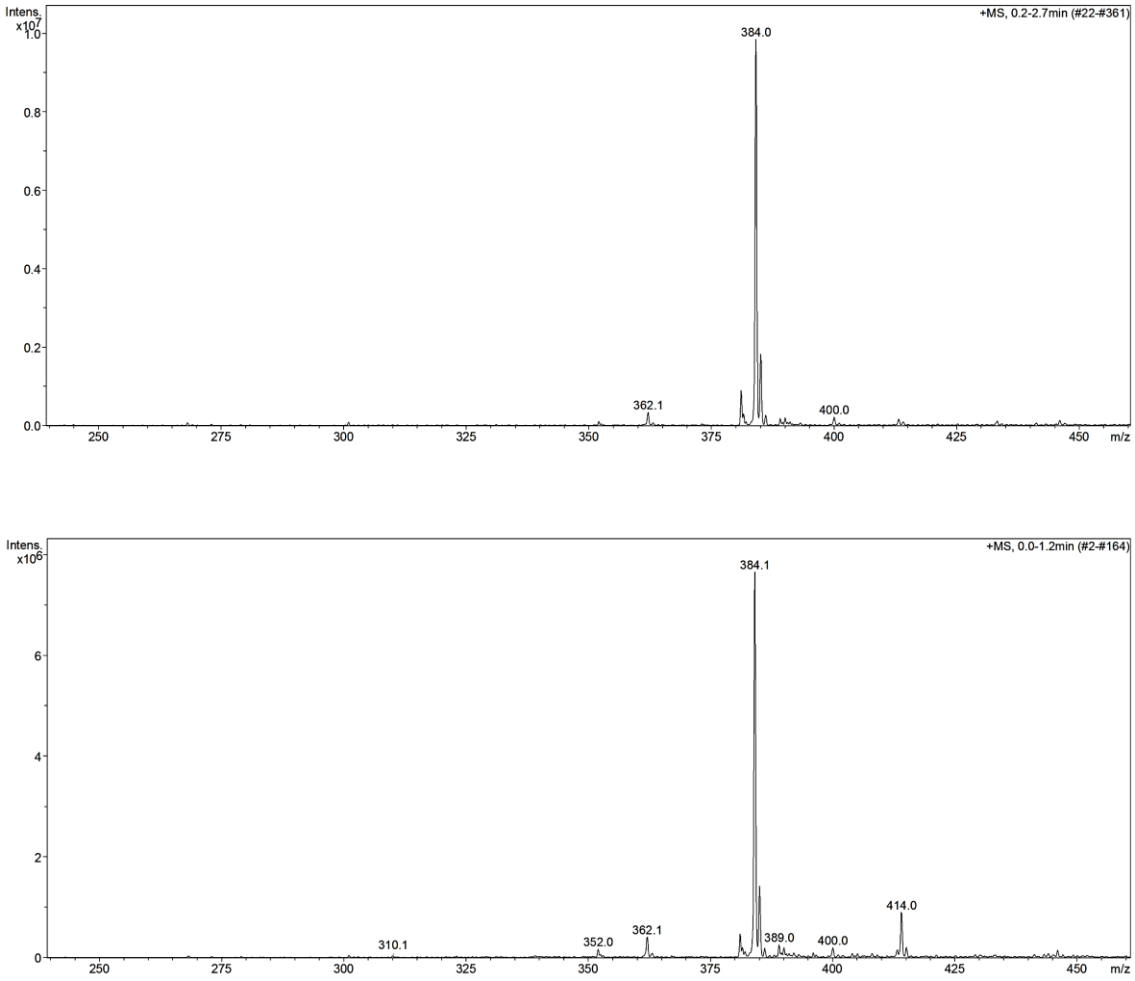

Figure 8 ESI-MS spectra of fresh (*Top*) and 200 kGy irradiated (*Bottom*) 0.44 mol/L HNO_3 solutions containing 0.15 mol/L PyTri-Tetraol solution.

A plausible degradation mechanism has been hypothesized on the basis of radiation chemistry literature [25, 27, 52]. In particular, the ligand degradation was supposed to be mainly caused by indirect radiolysis, due to reactions with radiolytic species of the diluent [53]. Furthermore, the lateral branches were hypothesized to be the weakest part of the ligand structure, while the aromatic moieties should reasonably be more radiation resistant. A first attack to the PyTri ligands could likely consist in hydrogen atom abstraction from the carbon atom in alpha position with respect to the triazolyl ring or from the one adjacent to the alcoholic group. Among all by-products generated by acidic solutions radiolysis, hydroxyl and, secondarily, nitrate radicals are the most reactive hydrogen abstracting agents [53-54]. Afterwards, the proposed degradation path entails

the cleavage of the N-$C_{alkylic}$ bond leading to lateral branch loss (by-product ***1*** of Figure 9 and Figure 10) or the addition of other radicals coming from diluent radiolysis (by-products ***2***, ***3***, ***4*** of Figure 9 and by-product ***2*** of Figure 10) [55]. The occurrence of multiple radical additions on a chain of the same ligand (by-products ***3*** of Figure 9) is an intriguing and surprising aspect from a statistical point of view, since just a minor amount of molecules seems to be damaged by the radiolytic process. Moreover, the site of radical insertion will be itself an additional site for further radical attacks competitive with the existing ones. In order to justify multiple damages on the same ligand, an intramolecular mechanism could be supposed. For instance, a peroxyradical attached to a weak site of the lateral chain could be able to abstract one hydrogen atom from another reactive site of the same branch.

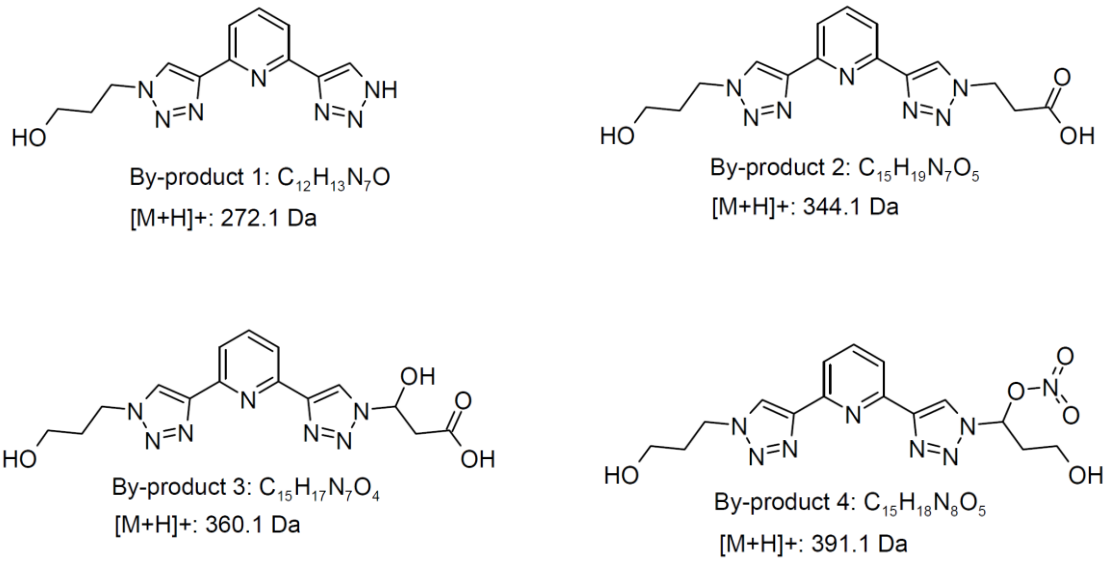

Figure 9 Hypothesized structures of main PyTri-Diol by-products (proton adducts). The nominal mass over charge values have been calculated considering the atomic weight of the most abundant natural isotopes for each element. These values have been rounded to the first decimal place for an easier comparison with the experimental spectra.

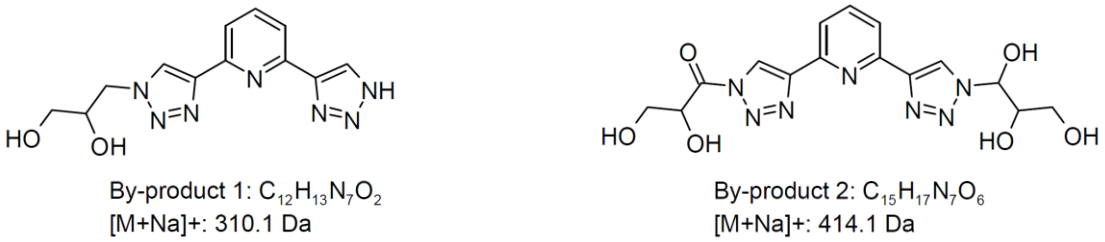

Figure 10 Hypothesized structures of main PyTri-Tetraol by-products (sodium adducts). The nominal mass over charge values have been calculated considering the atomic weight of the most abundant natural isotopes. These values have been rounded to the first decimal place for an easier comparison with the experimental spectra.

The identification of by-products structures is important not only in the case of stripping solvent recycling. In fact, one of the key issues to be addressed would be the accumulation of lipophilic by-products in the organic phase, since those may affect the system performances. The herein hypothesized by-products, owing to almost unaltered hydrophilicity and complexing site with respect to the pristine ligands, should preserve their extracting properties, in agreement with preliminary batch extraction data obtained with irradiated PyTri-Diol solutions [40]. Furthermore, these structures are consistent with FT-Raman results herein presented, since all radiolytic modification would affect just the lateral chains. In order to corroborate these outcomes, further investigations are ongoing, especially on by-product ***1***, since it is liable to be endowed with a slightly lower water solubility. In particular, HPLC-MS analyses of irradiated solutions are being carried out to confirm the hypothesized structures and obtain a semi-quantitative evaluation of pristine ligand and by-products in fresh, aged and irradiated solutions.

Conclusions

The herein studied hydrophilic PyTri ligands proved to be exceptional candidates for application to advanced MA Partitioning as they exhibited satisfactory radiolytic stability. Both the ligand degradation mechanism and the structures of the main degradation by-products were hypothesized on the basis of the analyses carried out on fresh, aged and gamma irradiated solutions. Preliminary confirmations were gathered

from ESI mass spectrometry. In particular, the ligand degradation was supposed to occur on the lateral chains rather than on the chelating unit and to be caused by indirect radiolysis due to interaction with diluent by-products. The aromatic core stability towards radiolysis was confirmed by FT-Raman spectroscopy. Furthermore, the herein identified by-products should preserve their hydrophilicity. These results are consistent with preliminary liquid-liquid extraction data obtained with irradiated PyTri-Diol solutions, since these by-products are expected to maintain MA selectivity, water solubility and, consequently, extraction performances as for pristine solutions. The demonstrated PyTri ligands radiolytic stability, besides promising MA selectivity and efficiency, further recommends their implementation in future processes.

Acknowledgements

This work has been supported by the EU-FP7 SACSESS project (Grant Number 323282), EU-H2020 GENIORS project (Grant number 755171), and the Italian Ministry of Education, University and Research. The DFT calculations were performed using Gaussian09 code and exploiting the computing resources awared by a public tender within the LISA Initiative promoted by Regione Lombardia and CINECA consortium.

The work was presented at the 2nd International Conference on Radioanalytical and Nuclear Chemistry (RANC 2019) held in Budapest (H) on May 5th-10th 2019.

References

[1] IAEA, TECDOC 1613 - Nuclear fuel cycle information system, International Atomic Energy Agency, Vienna, 2009.

[2] IAEA, Safety Standard 15 - Storage of spent nuclear fuel, International Atomic Energy Agency, Vienna, 2012.

[3] R. Herbst and P. Baron, Standard and advanced separation: PUREX processes for nuclear fuel reprocessing, in *Advanced Separation Techniques for Nuclear Fuel Reprocessing and Radioactive Waste Treatment*, United Kingdom, Woodhouse Publishing Ltd., 2011, pp. 141-175.

[4] IAEA, Technical Reports 435 - Implications of partitioning and transmutation in

radioactive waste management, International Atomic Energy Agency, Vienna, 2004.

[5] C. Poinssot, S. Bourg, N. Ouvrier, N. Combernoux, C. Rostaing, M. Vargas-Gonzalez, and J. Bruno, Assessment of the environmental footprint of nuclear energy systems. Comparison between closed and open fuel cycles, *Energy,* vol. 69, pp. 199-211, 2014.

[6] C. Poinssot, S. Bourg, and B. Boullis, Improving the nuclear energy sustainability by decreasing its environmental footprint. Guidelines from life cycle assessment simulations, *Prog. Nucl. Energ.,* vol. 92, pp. 234-241, 2016.

[7] IAEA, "TECDOC 1626 - Advanced reactor technology options for utilization and transmutation of actinides in spent nuclear fuel," International Atomic Energy Agency, Vienna, 2009.

[8] G. Modolo, A. Geist, and M. Miguirditchian, Minor actinide separations in the reprocessing of spent nuclear fuels: recent advances in Europe (Cap 10), in *Reprocessing and recycling of spent nuclear fuel*, Elsevier Ltd., 2015, pp. 245-287.

[9] A. V. Gelis, and G. J. Lumetta, Actinide Lanthanide Separation Process—ALSEP, *Ind. Eng. Chem. Res.,* vol. 53, pp. 1624-1631, 2014.

[10] M. Nilsson, and K. L. Nash, Review article: a review of the development and operational characteristics of the TALSPEAK process, *Solv. Extr. Ion Exch.,* vol. 25, pp. 665-701, 2007.

[11] Y. Koma, M. Watanabe, S. Nemoto, and Y. Tanaka, Trivalent lanthanide and actinide intra-group separation by solvent extraction with CMPO-complexant system, *J. Nucl. Sci. Techn.,* vol. 35, pp. 130-136, 1998.

[12] G. Modolo, A. Wilden, A. Geist, D. Magnusson, and R. Malmbeck, A review of the demonstration of innovative solvent extraction processes for the recovery of trivalent minor actinides from PUREX raffinate, *Radiochim. Acta,* vol. 100, pp. 715-725, 2012.

[13] R. Malmbeck, M. Carrot, B. Christiansen, A. Geist,, X. Heres, D. Magnusson, G. Modolo, C. Sorel, and R. Taylor, A. Wilden, EURO-GANEX, a process for the co-separation of TRU., in *Sustainable Nuclear Energy Conference*, Manchester (UK), 2014.

[14] A. Geist, G. Modolo, A. Wilden, P. Kaufholz, Minor actinide separation: simplification of the DIAMEX-SANEX strategy by means of novel SANEX processes, in *Proceedings of the International Conference on GLOBAL 2013 (Nuclear Energy at a Crossroads)*, Salt Lake City (USA), 2013.

[15] G. Modolo, A. Wilden, P. Kaufholz, D. Bosbach, and A. Geist, Development and demonstration of innovative partitioning processes (i-SANEX and 1-cycle SANEX) for actinide partitioning, *Prog. Nucl. Energy,* vol. 72, pp. 107-114, 2014.

[16] A. Wilden, G. Modolo, P. Kaufholz, F. Sadowski, S. Lange, M. Sypula, D. Magnusson, U. Müllich, A. Geist, and D. Bosbach, Laboratory-scale counter-current centrifugal contactor demonstration of an innovative SANEX process using a water soluble BTP, *Solv Extr. Ion Exch.,* vol. 33, pp. 91-108, 2015.

[17] S. A. Ansari, P. Pathak, P. K. Mohapatra, and V. K. Manchanda, Chemistry of diglycolamides: promising extractants for actinide partitioning, *Chem. Rev.,* vol.

112, pp. 1751-1772, 2012.

[18] Y. Sasaki, Y. Sugo, S. Suzuki, and S. Tachimori, The novel extractants, diglycolamides, for the extraction of lanthanides and actinides in HNO3/n-dodecane system, *Solvent Extr. Ion Exch.,* vol. 19, pp. 91-103, 2001.

[19] A. Geist, and G. Modolo, TODGA process development: an improved solvent formulation, in *Proceedings of the International Conference GLOBAL 2009 (The nuclear fuel cycle: Sustainable options & industrial perspectives)*, Paris, 2009.

[20] S. Bourg, ACSEPT - Actinide recycling by separation and transmutation - Final report, European Commission, 2012.

[21] P. Panak, and A. Geist, Complexation and Extraction of Trivalent Actinides and Lanthanides by Triazinylpyridine N-Donor Ligands, *Chem. Rev.,* vol. 113, p. 1199−1236, 2013.

[22] F. Lewis, L.M. Harwood, M.J. Hudson, A. Geist V.N. Kozhevnikov, P. Distler, and J. John, "Hydrophilic sulfonated bis-1,2,4-triazine ligands are highly effective reagents for separating actinides(iii) from lanthanides(iii) via selective formation of aqueous actinide complexes," *Chem. Sci.,* vol. 6, no. 8, pp. 4812-4821, 2015.

[23] A. Geist, U. Müllich, D. Magnusson, P. Kaden, G. Modolo, A. Wilden, and T. Zevaco, Actinide(III)/lanthanide(III) separation via selective aqueous complexation of actinides(III) using a hydrophilic 2,6-bis(1,2,4-triazin-3-yl)-pyridine in nitric acid, *Solvent Extr. Ion Exch.,* vol. 30, pp. 433-444, 2012.

[24] B. Mincher, G. Elias, L.R. Martin, and S.P. Mezyk, Radiation chemistry and the nuclear fuel cycle, *J. Radioanal. Nucl. Chem.,* vol. 282, p. 645–649, 2009.

[25] B. Mincher and S. Mezyk, Radiation chemical effects on radiochemistry: A review of examples important to nuclear power, *Radiochim. Acta,* vol. 97, p. 519–534, 2009.

[26] L. Berthon, and M. C. Charbonnel, Radiolysis of solvents used in nuclear fuel reprocessing, in *Ion exchange and solvent extraction: a series of advances*, Boca Raton (USA), CRC Press Taylor & Francis group, 2010, pp. 429-513.

[27] B. Mincher, G. Modolo, and S.P. Mezyk, Review article: the effects of radiation chemistry on solvent extraction 3: a review of actinide and lanthanide extraction, *Solvent Extr. Ion Exch.,* vol. 27, pp. 579-606, 2009.

[28] A. Pikaev, S.A. Kabakchi, and G.F. Egorov, Some radiation chemical aspects of nuclear engineering, *Radiat. Phys. Chem.,* vol. 31, pp. 789-803, 1988.

[29] S. C. Tripathi, and A Ramanujam, Effect of radiation induced physicochemical transformation on density and viscosity of 30% TBP-n-dodecane-HNO3 systems, *Sep. Sci. Technol,* vol. 38, pp. 2307-2326, 2003.

[30] E. Mossini, E. Macerata M. Giola, L. Brambilla, C. Castiglioni, and M. Mariani, Radiation-induced modifications on physico chemical properties of diluted nitric acid solutions within advanced spent nuclear fuel reprocessing, *J. Radioanal. Nucl. Chem.,* vol. 304, pp. 395-400, 2015.

[31] E. Mossini, E. Macerata, M. Giola, L. Brambilla, C. Castiglioni, and M. Mariani, Physico chemical properties of irradiated i-SANEX diluents, *Nukleonika,* vol. 60, pp. 893-898, 2015.

[32] Y. Sugo,Y. Izumi, Y. Yoshida, S. Nishijima, Y. Sasaki, T. Kimura, T. Sekine, and H. Kudo, Influence of diluent on radiolysis of amides in organic solution, *Rad. Phys. Chem.,* vol. 76, p. 794–800, 2007.

[33] Y. Sugo, Y. Sasaki, T. Kimura, T. Sekine, and H. Kudo, Radiolysis of TODGA and its effect on extraction of actinides ions, in *Proceeding of the International Conference GLOBAL 2005*, Tsukuba (J), 2005.

[34] Y. Sugo, Y. Sasaki, and S. Tachimori, Studies on hydrolysis and radiolysis of N,N,N9,N9-tetraoctyl-3-oxapentane-1,5-diamide, *Radiochim. Acta,* vol. 90, pp. 161-165, 2002.

[35] H. Galán, A. Núñez, A.G. Espartero, R. Sedano, A. Durana, and J. de Mendoza, Radiolytic Stability of TODGA: Characterization of Degraded Samples under Different Experimental Conditions, *Proc. Chem.,* vol. 7, p. 195–201, 2012.

[36] C. Zarzana, G.S. Groenewold, B.J. Mincher,, S.P. Mezyk, A. Wilden, H. Schmidt, G. Modolo, J.F. Wishart, and A.R. Cook, A Comparison of the γ-Radiolysis of TODGA and T(EH)DGA Using UHPLC-ESI-MS Analysis, *Solv. Extr. Ion Exch.,* vol. 33, p. 431–447, 2015.

[37] H. Galan, C.A. Zarzana, A. Wilden, A. Núñez,, H. Schmidt, R.J.M. Egberink, A. Leoncini,, J. Cobos, W. Verboom, G. Modolo G.S. Groenewold, and B.J. Mincher, Gamma-radiolytic stability of new methylated TODGA derivatives for minor actinide recycling, *Dalton Trans.,* vol. 44, pp. 18049-18056, 2015.

[38] G. Horne, S.P. Mezyk, N. Moulton, J.R. Peller, and A. Geist, Time-resolved and steady-state irradiation of hydrophilic sulfonated bis-triazinyl-(bi)pyridines – modelling radiolytic degradation, *Dalton Trans.,* vol. DOI: 10.1039/C9DT00474B, pp. 1-9, 2019.

[39] D. Peterman, A. Geist, B.J. Mincher, G. Modolo, H. Galán, L. Olson, and R. McDowell, Performance of an i-SANEX System Based on a Water-Soluble BTP under Continuous Irradiation in a γ-Radiolysis Test Loop, *Ind. Eng. Chem. Res.,* vol. 55, pp. 10427-10435, 2016.

[40] E. Macerata, E. Mossini, S. Scaravaggi, M. Mariani,, A. Mele, W. Panzeri, N. Boubals, L. Berthon, M.C. Charbonnel, F. Sansone, A. Arduini, and A. Casnati, Hydrophilic Clicked 2,6-Bis-triazolyl-pyridines Endowed with High Actinide Selectivity and Radiochemical Stability: Toward a Closed Nuclear Fuel Cycle, *J. Am. Chem. Soc.,* vol. 138, pp. 7232-7235, 2016.

[41] C. Wagner, E. Mossini, E. Macerata, M. Mariani, A. Arduini, A. Casnati, A. Geist, and P.J. Panak, Time-Resolved Laser Fluorescence Spectroscopy Study of the Coordination Chemistry of a Hydrophilic CHON [1,2,3-Triazol-4-yl]pyridine Ligand with Cm(III) and Eu(III), *Inorg Chem.,* vol. 56, pp. 2135-2144, 2017.

[42] A. Ossola, E. Macerata, E. Mossini, M. Giola, M.C. Gullo, A. Arduini, A. Casnati, M. Mariani, 2,6-Bis(1-alkyl-1H-1,2,3-triazol-4-yl)-pyridines: selective lipophilic chelating ligands for minor actinides, *J Radioanal Nucl Chem,* vol. 318, pp. 2013-2022, 2018.

[43] S. Bourg, P. Guilbaud, E. Mendes, C. Ekberg, et al., "SACSESS final report," 2016.

[44] E. Mossini, E. Macerata, A. Wilden, P. Kaufholz,, G. Modolo, N. Iotti, A. Casnati, A. Geist, and M. Mariani, Optimization and Single-Stage Centrifugal Contactor

Experiments with the Novel Hydrophilic Complexant PyTri-Diol for the i-SANEX Process, *Solvent Extraction and Ion Exchange*, vol. 36, p. 373–386, 2018.

[45] J. R. Taylor, An Introduction to Error Analysis: The Study of Uncertainties in Physical Measurements, Sausalito: University Science Books, 1996.

[46] A. Becke, Density-functional thermochemistry. III. The role of exact exchange, *J. Chem. Phys.*, vol. 98, pp. 5648-5652, 1993.

[47] C. Lee, W. Yang, and R.G. Parr, Development of the Colle-Salvetti correlation-energy formula into a functional of the electron density, *Phys. Rev. B*, vol. 37, pp. 785-789, 1988.

[48] R. Krishnan, J. S. Binkley, R. Seeger and J. A. Pople, Self-consistent molecular orbital methods. XX. A basis set for correlated wave functions, *J. Chem. Phys.*, vol. 72, pp. 650-654, 1980.

[49] Gaussian 09, Revision A.02, M. J. Frisch, G. W. Trucks, H. B. Schlegel, G. E. Scuseria, M. A. Robb, J. R. Cheeseman, G. Scalmani, V. Barone, G. A. Petersson, H. Nakatsuji, X. Li, M. Caricato, A. Marenich, J. Bloino, B. G. Janesko, R. Gomperts, B. Mennucci, H. P. Hratchian, J. V. Ortiz, A. F. Izmaylov, J. L. Sonnenberg, D. Williams-Young, F. Ding, F. Lipparini, F. Egidi, J. Goings, B. Peng, A. Petrone, T. Henderson, D. Ranasinghe, V. G. Zakrzewski, J. Gao, N. Rega, G. Zheng, W. Liang, M. Hada, M. Ehara, K. Toyota, R. Fukuda, J. Hasegawa, M. Ishida, T. Nakajima, Y. Honda, O. Kitao, H. Nakai, T. Vreven, K. Throssell, J. A. Montgomery, Jr., J. E. Peralta, F. Ogliaro, M. Bearpark, J. J. Heyd, E. Brothers, K. N. Kudin, V. N. Staroverov, T. Keith, R. Kobayashi, J. Normand, K. Raghavachari, A. Rendell, J. C. Burant, S. S. Iyengar, J. Tomasi, M. Cossi, J. M. Millam, M. Klene, C. Adamo, R. Cammi, J. W. Ochterski, R. L. Martin, K. Morokuma, O. Farkas, J. B. Foresman, and D. J. Fox, Gaussian, Inc., Wallingford CT, 2016.

[50] J. Tomasi, B. Mennucci, and R. Cammi, Quantum Mechanical Continuum Solvation Models, *Chem. Rev.*, vol. 105, pp. 2999-3094, 2005.

[51] A. Fermvik, C. Ekberg, S. Englund, M.R.S.J. Foreman, G. Modolo, T. Retegan, and G. Skarnemark, Influence of dose rate on the radiolytic stability of a BTBP solvent for actinide(III)/lanthanide(III) separation, *Radiochim. Acta*, vol. 97, pp. 319-324, 2009.

[52] B. Mincher, G. Modolo, and S.P. Mezyk, Review: The effects of radiation chemistry on solvent extraction 4: separation of trivalent actinides and considerations for radiation-resistant solvent systems, *Solvent Extr. Ion Exch.*, Vols. 415-436, p. 28, 2010.

[53] B. Mincher, G. Modolo, and S.P. Mezyk, Review article: the effects of radiation chemistry on solvent extraction: 1. Conditions in acidic solution and a review of TBP radiolysis, *Solvent Extr. Ion Exch.*, vol. 27, pp. 1-25, 2009.

[54] L. Wan, J. Peng, M.Z. Lin, Y. Muroya, Y. Katsumura, and H.Y. Fu, Hydroxyl radical, sulfate radical and nitrate radical reactivity towards crown ethers in aqueous solutions, *Rad. Phys. Chem.*, vol. 81, pp. 524-530, 2012.

[55] G. Buxton, C.L. Greenstock, W.P. Helman and A.B. Ross, Critical review of rate constants for reactions of hydrated electrons, hydrogen atoms and hydroxyl radicals (OH/O–) in aqueous solution, *J. Phys. Chem. Ref. Data*, vol. 17, p. 513–886, 1988.